Direct Measurements of Single-Event Burnout Current Induced by Neutron Irradiation in a 1200 V Fast Recovery Diode

Hikaru Nakamoto[†], Jun Furuta[‡], Michitarou Yabuuchi[†††], Hironori Sakamoto[†††], Ryuichi Nakajima[†], Kazutoshi Kobayashi[†], Makoto Sakai[††††] [†††††] and Shigetaka Kumashiro[†††]

† Dept. of Electronics, Kyoto Institute of Technology, Japan

‡ Dept. of Info. and Comm. Eng., Okayama Prefectural University, Japan

[†††] Renesas Electronics Corporation, Japan

[††††] Gunma University Heavy Ion Medical Center (GHMC), Japan

[†††††] Faculty of Medical Sciences, Kyushu University, Japan

***Abstract*—In this paper, we conducted neutron irradiation experiments and measured Single Event Burnout (SEB) current in a Fast Recovery Diode (FRD) using an oscilloscope. The results suggest that SEB current depends not only on the applied voltage but also on the Linear Energy Transfer (LET) of secondary ions. Device simulations revealed that the conventional models could not reproduce the measured SEB current, but increasing the initial charge amount and impact ionization coefficient led to improved consistency. From cross-sectional analysis, reducing parallel capacitance suppressed burnout, while aluminum electrode penetration, silicon melting marks, and cracks due to thermal stress were observed.**

***Index Terms*—Single Event Burnout (SEB), current, device simulations, neutron irradiation, impact ionization.**

I. Introduction

High reliability is essential for power semiconductors in advanced industrial applications. However, some devices are highly susceptible to radiation-induced degradation, requiring radiation-resistant designs. Single Event Burnout (SEB) occurs when a radiation particle strikes a device in the off state, generating electron-hole pairs. This leads to a localized current pulse increase due to impact ionization, ultimately causing unrecoverble permanent failure. Thus, improving SEB resistance is critical.

Understanding SEB failure mechanisms and optimizing device design is a key for enhancing SEB resistance. While cross-sectional analyses of SEB-induced damage are already discussed in [1], [2], studies on failure processes are not well discussed. Device simulations are effective for SEB evaluation as they allow the analysis of physical parameters within the device. However, they do not always fully reproduce the device response during SEB occurrence. The lack of experimental SEB current measurements further complicates model validation and failure analysis. Therefore, comparing simulations with experimental data is essential.

In this study, we measured the SEB current using an oscilloscope to capture the initial current increase immediately after radiation strikes. We also examined its dependence on voltage and parallel capacitance, compared experimental results with simulations, and conducted a cross-sectional analysis of SEB-induced damage.

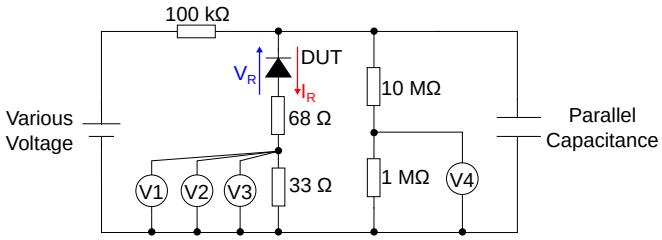

Fig. 1: Measurement circuit for the SEB current.

II. Measurement Setups

We measured the SEB current using an oscilloscope with the measurement circuit shown in Fig. 1. To clarify SEB occurrence conditions and current characteristics, we evaluate the effects of voltage sweep and variations in parallel capacitance. Since parallel capacitance plays a significant role in SEB occurrence [3], different capacitance values are set to assess its specific impact on SEB behavior. To limit the power supply current, a high resistance is inserted into the circuit to remove the supply current contribution to SEB occurrence [4]. A 1200 V-rated Si Fast Recovery Diode (FRD) is used as the measurement target. we evaluated SEB in an FRD under reverse bias. Since the influence of carriers injected under forward bias is absent, the evaluation focuses purely on the carrier multiplication process induced by secondary ions. During the measurement, a reverse voltage is applied to the FRD, and the SEB current I_R is captured using an oscilloscope. To accommodate the wide SEB current range, three measurement probes (V1, V2, and V3) with different ranges are connected to the same node. Additionally, V4, which is in parallel with the applied voltage V_R, is monitored to detect voltage drop during SEB occurrence.

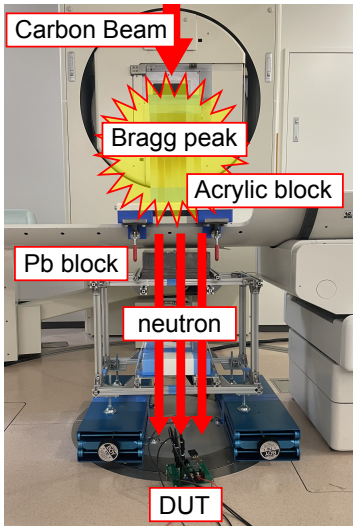

Fig. 2: Measurement setup using neutrons generated by the clinical carbon beam. The Pb block is used for charged particle shielding.

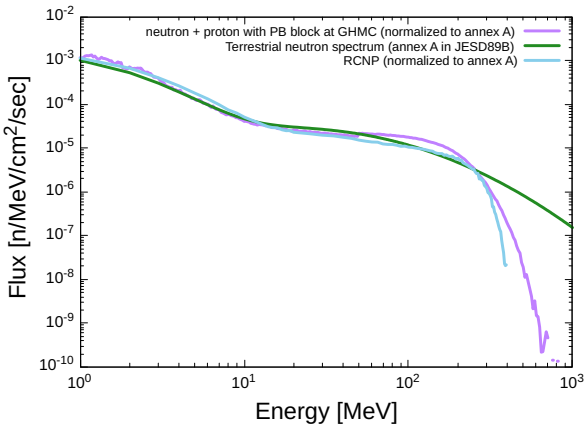

Fig. 3: Neutron energy spectrum at the DUT installation site, normalized by the number of neutrons above 1 MeV and protons above 50 MeV.

We conducted neutron irradiation experiments using a white neutron beam at the Research Center for Nuclear Physics (RCNP) [5] and high energy neutrons created by a clinical carbon beam at Gunma University Heavy Ion Medical Center (GHMC) [6]. The overall measurement setup at GHMC is shown in Fig. 2. Secondary particles, primarily neutrons, protons, and alpha particles, are generated near the Bragg peak by irradiating an acrylic block with a clinical carbon beam. SEB occurs exclusively due to the high-energy neutrons [7], making the effects of low-energy protons and alpha particles negligible. The generated neutrons are then irradiated onto the DUT. The neutron energy spectrum at the DUT was calculated using PHITS (Particle and Heavy Ion Transport code System) [8]. The neutron spectra at RCNP, GHMC, and in terrestrial environments [9] are shown in Fig. 3.

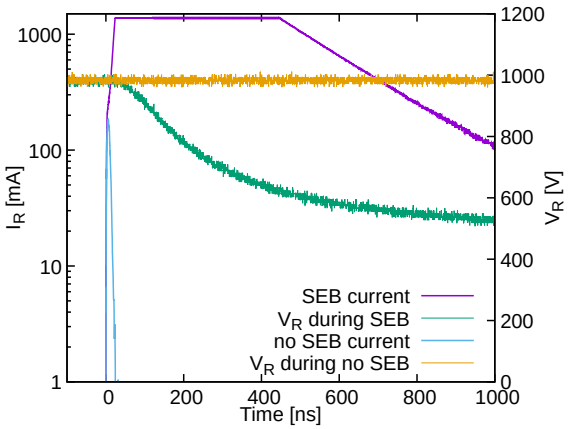

Fig. 4: Current for SEB occurrence and non-occurrence cases, along with voltage variation during SEB, measured at GHMC with V_R = 980 V and a parallel capacitance of 2 nF.

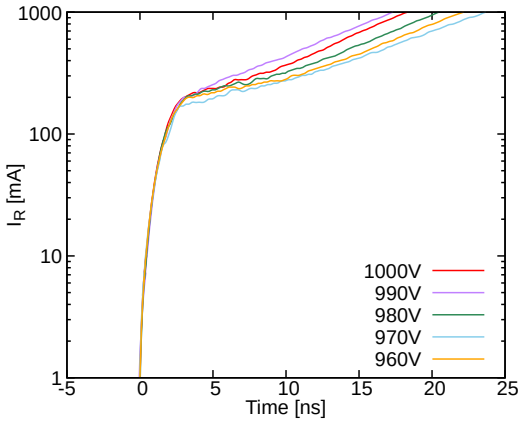

Fig. 5: SEB current during a voltage sweep from V_R = 960 V to 1000 V with a parallel capacitance of 2 nF, measured at GHMC.

III. Measurements Results

Fig. 4 shows the SEB current, along with the corresponding voltage change and the current when SEB does not occur. These measurements were conducted under the conditions of V_R = 980 V and a parallel capacitance of 2 nF. A voltage drop of V_R during SEB is used as the criterion for SEB occurrence. Due to specifications of the oscilloscope, current above 1400 mA cannot be recorded. V_R begins to decrease after the current reaches 1000 mA, suggesting that damage formation starts at this threshold. The subsequent voltage drop likely corresponds to the expansion of the damage region.

Fig. 5 shows the SEB current measured from V_R = 960 V to 1000 V. The time when I_R reaches 1 mA is set as 0 ns, with a parallel capacitance of 2 nF in all cases. Up to 2.5 ns, the current rise is independent of voltage, showing similar behavior across all V_R with a little variation in the initial current. However, after 2.5 ns, differences in the current in-

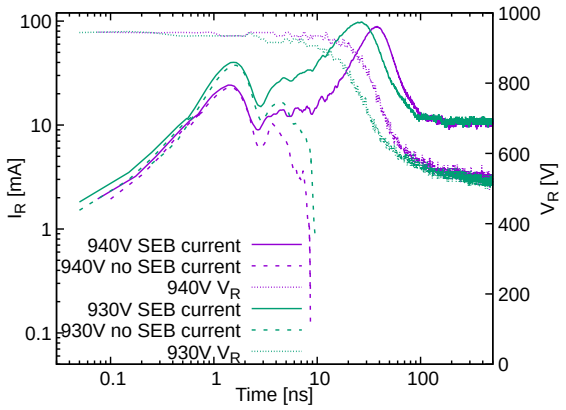

Fig. 6: SEB current for V_R = 940 V and 930 V with no parallel capacitance, including both SEB occurrence and non-occurrence cases, along with voltage variation during SEB, measured at RCNP.

crease were observed depending on the voltage. While a higher voltage should shorten the breakdown time due to increased electric field, this trend was not seen in the measurements. This discrepancy is likely due to the Linear Energy Transfer (LET) of secondary ions generated by neutrons. Higher LET increases carrier generation, reducing the time to reach 1000 mA [10]. Thus, under a narrow voltage sweep range, both voltage variation and LET significantly influence the SEB current.

Fig. 6 shows the measured SEB current for V_R = 940 V and 930 V with no parallel capacitance. The initial current peak remained the same regardless of SEB occurrence. However, among the cases where the same initial current peak around 1.5 ns was observed, approximately 10% exhibited a subsequent current increase leading to SEB. A detailed examination of the SEB current reveals that after the initial current peak, the current temporarily decreases and rises with repeated fluctuations. Such behavior suggests that excessive impact ionization occurs probabilistically and sporadically, leading to SEB only when its frequency is sufficiently high. Additionally, similar fluctuations are observed even in the current waveforms where SEB did not occur, suggesting that while impact ionization arises, SEB may be avoided if its intensity is insufficient.

IV. Discussion

A. SEB Current Reproduction in Device Simulation

Using PHITS [8], we calculate the maximum LET and the corresponding track length of neutron-induced secondary ions within the FRD. TABLE I shows the maximum LET values obtained for different track lengths. Among these, the track length of 30 μm and the maximum LET of 1.5 MeV-cm^2/mg are identified as the combination with the highest charge generation potential. The amount of generated charge is estimated as the product of the LET and the track length. Using this combination, a comparison between the device simulation and the experimental measurements was conducted.

TABLE I: Maximum LET values of neutron-induced secondary ions in the FRD for different track lengths, calculated using PHITS.

Track Length [um]	Maximum LET [MeV-cm^2/mg]
0.5	3.5
1	4.5
6	5.5
10	3.5
16	2.5
20	1.5
30	1.5
50	0.5

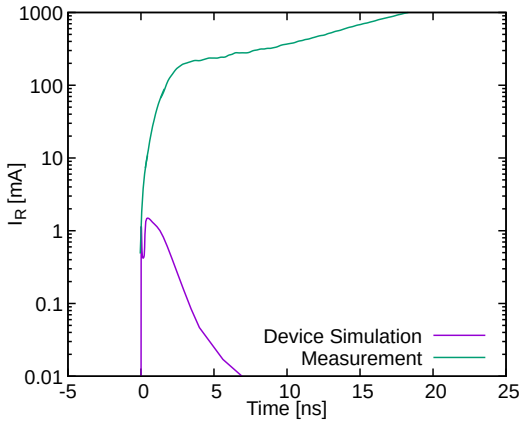

Fig. 7: Comparison between the experimental results and the device simulation with conventional settings. In both experimental and simulation conditions, V_R is set to 1000 V.

The simulation is performed using Sentaurus by Synopsys with a device model replicating the impurity concentration and structure of the FRD. The current during SEB occurrence is evaluated by simulating heavy ion injection. Both experimental and simulation conditions are set to V_R = 1000 V. Fig. 7 compares the measured and the simulated results, showing that the peak current in the simulation is significantly lower than that in experiments, failing to accurately reproduce the SEB current. This indicates that conventional device simulations cannot quantitatively reproduce the SEB current.

To reproduce the excessive impact ionization state, which occurs with low probability as suggested by Fig. 6, the initially generated charge is increased by a factor of 30, and the electric field sensitivity of the impact ionization coefficient is increased by a factor of 1.4. As a result, the simulation current successfully matches the experimental current, as shown in Fig. 8. The physical validity of this simulation condition requires further investigation. However, given that the SEB occurrence rate is significantly lower than the incidence probability of secondary ions and increases exponentially with V_R, sporadic excessive impact ionization is likely to play a crucial role in SEB.

B. Cross-Sectional Analysis of SEB-Induced Damage Region

By using the measurement circuit in this study, SEB-induced thermal melting was suppressed by removing the parallel

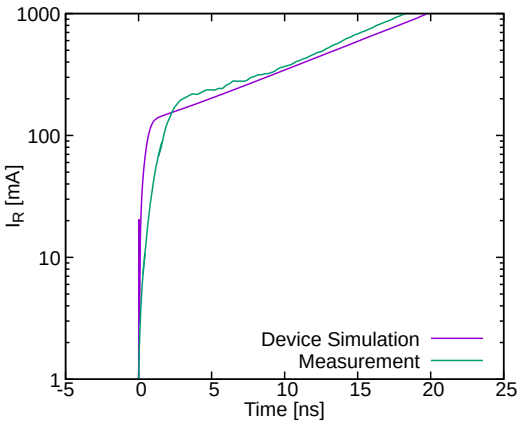

Fig. 8: Comparison between the experimental results and the proposed device simulation when the initial generated charge is increased by a factor of 30 and the electric field sensitivity of the impact ionization coefficient is increased by a factor of 1.4. Both experimental and simulation conditions have V_R set to 1000 V.

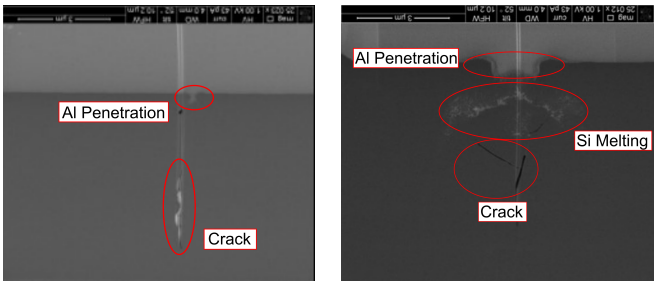

(a) No parallel capacitance. (b) A parallel capacitance of 2 nF.

Fig. 9: Cross-sectional image of SEB-induced damage at a voltage of 1000 V.

capacitance. Cross-sectional analysis was conducted on two types of SEB-induced damage, identified via the Optical Beam Induced Resistance Change (OBIRCH) method [11] and observed by using an electron microscope. Fig. 9a (no parallel capacitance) and Fig. 9b (2 nF) compare the cross-sectional damage under 1000 V. Both conditions resulted in permanent FRD failure, but the no parallel capacitance case exhibited reduced burnout damage region compared to 2 nF. The 2 nF condition showed significant aluminum penetration, silicon melting, and thermal stress-induced cracks, whereas at no parallel capacitance, these effects were mitigated, and aluminum penetration was noticeably smaller. Suppressing thermal melting allows for a clearer analysis of the failure process and the measurement of the minimum failure current, contributing to thermal simulation accuracy improvement.

V. Conclusion

In this study, we measured the SEB current using an oscilloscope. The results indicate that SEB current depends on both the applied voltage and the LET of secondary ions, with excessive impact ionization playing a key role. Device simulations revealed that conventional models could not fully reproduce the measured SEB current. However, adjusting the initial charge amount and impact ionization coefficient improved the agreement with the experimental results. Cross-sectional analysis showed that reducing the parallel capacitance can suppress burnout, while Al electrode penetration, Si melting marks, and thermal stress-induced cracks were observed.

Future research should further analyze the relationship between SEB occurrence probability and impact ionization to refine the physical validity of the simulation model. Additionally, enhancing SEB damage suppression will deepen the understanding of the failure mechanism.

VI. Acnowledgement

The authors would like to thank to Research Center for Nuclear Physics (RCNP), Osaka University for our white neutron beam experiments. This work was supported through the activities of d-lab. VDEC, The university of Tokyo, in collaboration with NIHON SYNOPSYS G.K..

References

[1] T. Shoji, S. Nishida, K. Hamada, and H. Tadano, "Observation and analysis of neutron-induced single-event burnout in silicon power diodes," *IEEE Transactions on Power Electronics*, vol. 30, no. 5, pp. 2474–2480, 2015.

[2] S. Kuboyama, C. Kamezawa, N. Ikeda, T. Hirao, and H. Ohyama, "Anomalous charge collection in silicon carbide schottky barrier diodes and resulting permanent damage and single-event burnout," *IEEE Transactions on Nuclear Science*, vol. 53, no. 6, pp. 3343–3348, 2006.

[3] T. A. Fischer, "Heavy-ion-induced, gate-rupture in power mosfets," *IEEE Transactions on Nuclear Science*, vol. 34, no. 6, pp. 1786–1791, 1987.

[4] "MIL-STD-750E," Test method standard - Test methods for semiconductor devices, 2006.

[5] C. W. Slayman, "Theoretical correlation of broad spectrum neutron sources for accelerated soft error testing," *IEEE Transactions on Nuclear Science*, vol. 57, no. 6, pp. 3163–3168, 2010.

[6] R. Nakajima, S. Sugitani, H. Sugisaki, T. Ito, J. Furuta, K. Kobayashi, and M. Sakai, "An approach to neutron-induced ser evaluation using a clinical 290 mev/ u carbon beam and particle transport simulations," in *2024 IEEE International Reliability Physics Symposium (IRPS)*, 2024, pp. 1–4.

[7] D. Oberg, J. Wert, E. Normand, P. Majewski, and S. Wender, "First observations of power mosfet burnout with high energy neutrons," *IEEE Transactions on Nuclear Science*, vol. 43, no. 6, pp. 2913–2920, 1996.

[8] T. Sato, Y. Iwamoto, S. Hashimoto, T. Ogawa, T. Furuta, S. Abe *et al.*, "Recent improvements of the particle and heavy ion transport code system – phits version 3.33," *J. Nucl. Sci. Technol.*, vol. 61, no. 1, pp. 127–135, 2024.

[9] "Measurement and reporting of alpha particle and terrestrial cosmic ray-induced soft errors in semiconductor devices," in *JEDEC SOLID STATE TECHNOLOGY ASSOCIATION*, October 2006.

[10] A. Sengupta, D. R. Ball, A. L. Sternberg, S. Islam, A. S. Senarath, R. A. Reed, M. W. McCurdy, E. X. Zhang, J. M. Hutson, M. L. Alles, J. M. Osheroff, B. Jacob, C. W. Hitchcock, S. Goswami, R. D. Schrimpf, K. F. Galloway, and A. F. Witulski, "Let and voltage dependence of single-event burnout and single-event leakage current in high-voltage sic power devices," *IEEE Transactions on Nuclear Science*, vol. 71, no. 4, pp. 809–815, 2024.

[11] K. Nikawa, "Optical beam induced resistance change (obirch): overview and recent results," in *The 16th Annual Meeting of the IEEE Lasers and Electro-Optics Society, 2003. LEOS 2003.*, vol. 2, 2003, pp. 742–743 vol.2.